Ecological Complexity 31 (2017) 78–87

Contents lists available at ScienceDirect

Ecological Complexity

journal homepage: www.elsevier.com/locate/ecocom

Original Research Article

Epidemiological landscape models reproduce cyclic insect outbreaks

Hedvig K. Nenzén [a,b,*], Elise Filotas [c], Pedro Peres-Neto [a], Dominique Gravel [b]

[a] Canada Research Chair in Spatial Modeling and Biodiversity, Département des Sciences Biologiques, Université du Québec à Montréal, CP 8888, Succ. Centre Ville, Montréal, Québec H3C 3P8, Canada
[b] Canada Research Chair in Integrative Ecology, Département de Biologie, Faculté des Sciences, Université de Sherbrooke, 2500, boulevard de l'Université, Sherbrooke, Québec J1K 2R1, Canada
[c] Center for Forest Research, Département Science et Technologie, Université du Québec, Téluq, 5800 rue Saint-Denis, Montréal, Québec H2S 3L5, Canada

ARTICLE INFO

Article history:
Received 7 October 2016
Received in revised form 13 April 2017
Accepted 17 April 2017
Available online 5 May 2017

Keywords:
Insects
Epidemics
Landscape ecology
Modeling

ABSTRACT

Forest insect outbreaks can have large impacts on ecosystems and understanding the underlying ecological processes is critical for their management. Current process-based modeling approaches of insect outbreaks are often based on population processes operating at small spatial scales (i.e. within individual forest stands). As such, they are difficult to parameterize and offer limited applicability when modeling and predicting outbreaks at the landscape level where management actions take place. In this paper, we propose a new process-based landscape model of forest insect outbreaks that is based on stand defoliation, the Forest-Infected-Recovering-Forest (FIRF) model. We explore both spatially-implicit (mean field equations with global dispersal) and spatially-explicit (cellular automata with limited dispersal between neighboring stands) versions of this model to assess the role of dispersal in the landscape dynamics of outbreaks. We show that density-dependent dispersal is necessary to generate cyclic outbreaks in the spatially-implicit version of the model. The spatially-explicit FIRF model with local and stochastic dispersal displays cyclic outbreaks at the landscape scale and patchy outbreaks in space, even without density-dependence. Our simple, process-based FIRF model reproduces large scale outbreaks and can provide an innovative approach to model and manage forest pests at the landscape scale.

1. Introduction

Many species undergo massive outbreaks, fluctuations in population densities that occur synchronously in multiple locations, sometimes with surprising regularity in time (Elton, 1924; Liebhold et al., 2004). Forest insects in particular have large recurrent population oscillations, such as spruce budworm, larch budmoth, gypsy moth, autumnal/winter moth (Bjørnstad et al., 2002; Ims et al., 2004; Johnson et al., 2006; Williams and Liebhold, 2000; Tenow et al., 2012). Landscape-wide outbreaks of forest insects produce large-scale defoliation and mortality of host tree species, some extending over millions of hectares. Insect outbreaks modify forest succession and composition, alter nutrient cycling, with profound consequences on ecosystem functions and services (Boyd et al., 2013; McCullough et al., 1998). These damages have led forest managers in affected territories to seek effective intervention strategies that dampen their negative consequences and impede their propagation over large expanses.

Numerous hypotheses to explain outbreaks of forest insects have been explored and/or implemented in what can be broadly divided into statistical and process-based models (Cuddington et al., 2013). Statistical (phenomenological, static, empirical) models describe and reproduce outbreaks from the characteristics of their distribution (e.g. outbreak location and duration, James et al., 2010). Because these models are derived from data sampled during past conditions, they may have limited ability to forecast the occurrence of outbreaks in changing management and weather conditions (Gustafson, 2013). On the other hand, process-based models (dynamic, mechanistic) are developed from ecological hypotheses about the plant-insect dynamics (Bjørnstad and Grenfell, 2001). Because they are based on ecological processes, these models are thought to be able to predict beyond sampled data (Cooke et al., 2007; Evans et al., 2012).

Most process-based models of insect outbreaks generally represent dynamics of population densities. The design, parameterization and validation of process-based models with local population-level dynamics presents two major difficulties: (1) it requires comprehensive knowledge of the many processes operating at the local population level, and (2) it requires estimates

* Corresponding author.

http://dx.doi.org/10.1016/j.ecocom.2017.04.004
1476-945X/

of insect densities. However, these requirements are difficult to meet because relationships between stand-scale processes and insect population dynamics are mostly studied in single locations (e.g. Royama, 1984). Moreover, if a phenomena is studied at the wrong scale, the resulting conclusions may be weak or unreliable (Meentemeyer et al., 2012; Peters et al., 2004). To circumvent this lack of data and avoid scale-mismatch, we investigate a landscape-scale model that is independent of small-scale within-stand population processes. The model represents forest stands with three possible states: *F*, a forest stand at endemic insect densities, *I*, an infested/infected stand at epidemic insect densities, and *R*, a recovering stand in which forest regenerates following defoliation. The model exploits the fact that stand densities of forest insects show extreme fluctuations between endemic and epidemic periods, corresponding to the forest or infected states (Royama, 1984) respectively. We refer to this model as a FIRF landscape model and explore its capacity to reproduce the macroscopic properties of insect outbreaks.

The FIRF dynamic model of forest insect outbreaks follows the frameworks of metapopulation and epidemiological models. In metapopulation models, local populations can be present or absent, and regional persistence depends on dispersal (Levins, 1969; Hanski, 1998). This wide class of models are also called disturbance-recovery, state-transition, occupancy and patch-dynamic models and have been applied to various ecological situations, such as fires (Malamud et al., 1998; Staver and Levin, 2012; Keane et al., 2015), mussel bed colonization (Guichard et al., 2003) and semi-arid vegetation (Kéfi et al., 2007). Similarly, epidemiological models consider hosts (analogous to local populations in the metapopulation models) as infected or not, and do not track the density of infectious agents within each host. Epidemiology provides a tractable theory to understand epidemics and applies vaccines against human, animal and plant diseases (Kermack and McKendrick, 1927; Riley, 2007; Keeling and Rohani, 2008). Epidemiological models in which one patch represents one host have been used to represent the dynamics of theoretical (Rhodes et al., 1998; Fuentes et al., 1999; Filipe and Maule, 2004; Neri et al., 2011) and real epidemics (Kleczkowski et al., 1997; Eisinger and Thulke, 2008; Neri et al., 2011; Filipe et al., 2012). Metapopulation and epidemiological models are related because both deal with the absence or presence of a species in multiple locations, not local densities (Earn et al., 1998; Grenfell and Harwood, 1997; Rhodes et al., 1998). However, to our knowledge, epidemiological and metapopulation landscape models have rarely been applied to study cyclic forest insect landscape epidemics (Keane et al., 2015).

The goal of this paper is to build a simple, macroscopic and process-based epidemiological model to explore the consequences of dispersal on insect outbreaks. Metapopulation and epidemiological models easily map onto the landscape dynamics of forest insects and present certain advantages over population models. Focusing on forests instead of insects matches the type of large-scale data surveyed regarding the effects of outbreaks (tree defoliation), not the density of insects (Gray, 2008; Bouchard and Auger, 2014). Simplifying the model by using a lower modeling resolution is computationally efficient and requires fewer parameters. Just like epidemiological models do not model virus densities within infected individuals, modeling the number of insects is too fine-scale to be informative at a landscape-level. The desired output for forest management is the proportion of forest stands that are affected, and for that reason we model forests instead of insects. Using metapopulation and epidemiology theory would allow forest managers to use insights from those fields, for example that the strength and type of disease transmission are essential determinants of distribution and epidemics (Hanski, 1998; Riley, 2007; Keeling et al., 2003).

We study two versions of our model: a spatially-explicit version in which insects disperse among forest stands arranged on a grid, and a spatially-implicit version with global dispersal (between all forest stands regardless of location). We define outbreaks as sudden peaks in the proportion of infected stands at the regional scale. Comparing both versions reveals how limited dispersal distance of insects contributes to outbreak dynamics at the landscape scale. Our goal is to understand the conditions at which outbreaks occur, and to characterize the spatiotemporal signature of outbreaks emerging from between-stand insect dispersal. We first describe the rationale of the modeling approach, here inspired by the ecological dynamics of the spruce budworm, a major defoliator of North American forests. We then provide a detailed description of the spatially-implicit and spatially-explicit stochastic dispersal versions of the model. We explore the structural and parameter sensitivity of the model to understand the conditions required for outbreaks to occur. We specifically answer three questions; (1) Which dispersal parameters are required to produce outbreaks? (2) Which dispersal parameters determine cyclic outbreaks? (3) Which dispersal parameters determine the spatial distribution of outbreaks?

2. Methods

We develop a general model of defoliating insect dynamics at the landscape scale, whose implementation is largely inspired by the extensive literature on the spruce budworm *Choristoneura fumiferana*. Spruce budworm outbreaks have occurred with intervals of around 30 years during the last 500 years (Morin et al., 2007; Boulanger et al., 2012), and have profoundly structured the dynamics of North American forests (Fleming, 2000). Budworm outbreaks damage around 15% of the surface of Canadian forests during each outbreak (NFS, 2013), representing large revenue losses. We first provide a general overview of the model to lay out the underlying ecology, and then detail more specific information about its implementation.

2.1. FIRF model overview

The modeling unit is a forest stand and each stand can be in one of three possible states: *F* forest, *I* infected defoliated forest, and *R* recovering forest (Fig. 1). These stands are represented on a continuous lattice where each cell corresponds to a stand. We adapt the epidemiological Susceptible-Infected-Recovering-Susceptible model (*SIRS*, Hethcote, 1976; Anderson and May, 1979) to insect outbreaks that have a dispersing pest affecting a stationary regenerating resource. Note that in our model each stand can only take one value, in contrast to population-based lattice models that simulate the density of trees in different states in each stand. The *F*

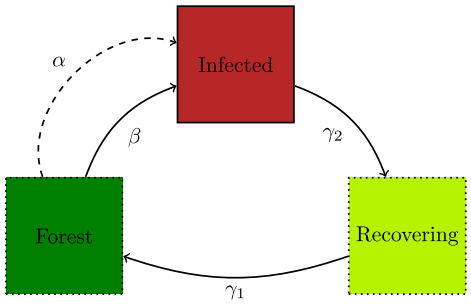

Fig. 1. Schema of the transitions between the three different states of the Forest-Infected-Recovering-Forest model of forest insect outbreaks. β is the probability of spontaneous infections, α is the probability of infection spread, γ_2 is the probability of infection dieback, γ_1 is the probability of forest recovery to mature, susceptible forest (also see Table S1).

forest and I infected states correspond to endemic and epidemic densities of spruce budworm, whose densities fluctuate over several order of magnitudes (Royama, 1984). During endemic periods the species is described as rare, while during epidemics there are hundreds of feeding larvae per kilogram of host foliage (Régnière et al., 2013). In our model, mature forest stands F have an endemic budworm density which does not cause stand-scale defoliation. Infected stands I have an epidemic density of insects and display signs of defoliation. There is a recovering, immature forest state R representing regeneration taking place after defoliation (Erdle and Maclean, 1999). Previous studies have shown that infection occurs more in mature forests (>60 years) compared to immature forests (85% vs. 42%, respectively, for the main host of spruce budworm (Balsam fir) from 1914 to 1979 outbreaks in Eastern North American temperate forests, Maclean and Olstaff, 1989). For simplicity, we limit our investigation to only one type of host forest and have omitted unpalatable deciduous trees. The budworm completes its life cycle in one year, which we equate with one time step in the model.

A mature (susceptible) forest stand F can become infected I in two ways (Fig. 1). This is similar to epidemiological models where disease can be acquired by a primary, 'index' infection from an external source, or from a secondary transmission from an already infected host (Rhodes et al., 1998). First, a forest stand can be infected seemingly spontaneously when low densities transition to high densities even when no neighboring stands are infected, a so-called 'epicenter' (Hardy et al., 1983; Cooke et al., 2007). The probability of a spontaneous infection is set by the parameter β. The cause of a local infection is difficult to identify, and many studies have focused on linking their presence to factors such as weather, long-distance dispersal and natural enemy release (Blais, 1958; Royama et al., 2005). We explore the model both with and without spontaneous infection.

Second, a transition from forest F to infected I in one stand can occur due to insect dispersal from neighboring infested stands and successive establishment, with probability α. After an epicenter has occurred, dispersal is an important driver of spruce budworm dynamics (Williams and Liebhold, 2000; Cooke et al., 2007). Most dispersal occurs between neighboring stands. For example, during the 2003–2011 northern Quebec outbreak, dispersal events occurred 10–80 km from an infected location (Bouchard and Auger, 2014). Although the budworm may be capable of occasional long-distance dispersal (Greenbank, 1980), this is difficult to quantify. We consider the length of a single stand to be 1–10 km, and we set the radius of dispersal to two adjacent stand. Dispersal therefore occurs from the 24 closest stands.

Dispersal of forest insect pests is often density-dependent, and more specifically driven by densities in the origin or arrival stand (Bowler and Benton, 2005). Mating success for instance is lower at endemic population densities due to an Allee effect (Régnière et al., 2013). We do not track insect densities explicitly and consequently indirectly model density-dependent dispersal using the proportion of infected stands in the neighborhood of a target stand as a proxy of density. Dispersal may be affected by insect densities around the stand where dispersal originates from (i.e. emigration), or by densities around the stand where propagules arrive (i.e. immigration). Egg-laying females in infected high-density stands emigrate to uninfected stands to avoid food shortage (Royama, 1984; Nealis and Régnière, 2004; Régnière et al., 2013). Alternatively, there is a lower probability of successful mating and immigration in arrival stands surrounded by uninfected stands. We explore landscape consequences of the Allee effect in the spatially-implicit model, and the consequences of emigration- and immigration-driven dispersal in the spatially-explicit model.

Emigration We consider that probability of emigration from the infected origin stand depends on the number of infected stands around the origin stand. As such, the probability of dispersal from the origin stand depends on the number of infected stands in the neighborhood centered around that stand.

Immigration Alternatively, we consider that the probability of a successful immigration is affected by the number of infected stands around the arrival stand. As such, the probability of dispersal to an arrival stand depends on the number of infected stands in its neighborhood.

Once a stand is infected, the infected forest has a probability γ_2 of dying and transitioning to a recovering forest stand. We assume that infection is lethal, meaning that once a forest stand has become infected, it cannot return to the mature forest state. We omit for simplicity trees that may be weakly defoliated and survive a spruce budworm outbreak episode (MacLean, 1980). We assume that budworm is the only source of forest stand mortality in the model and disregard senescence, especially because old-growth forests can also show budworm infection.

Recovering stands reach maturity with probability γ_1. The boreal forest has aerial seed dispersal and seedlings continuously establish underneath the forest canopy. Boreal coniferous species, at least balsam fir, white and black spruce, have abundant natural regeneration (Bergeron et al., 1995) and therefore we omit spatially explicit dispersal constraints for trees. Therefore recovery to mature forest is a non-spatial process (well-mixed, Pascual and Guichard, 2005) that depends only on the total proportion of recovering forest in the landscape, $\gamma_1 R$.

2.1.1. Spatially-implicit model formulation

We now translate the ecological description of the forest-insect dynamics given above to a spatially-implicit model with global dispersal. It is a mean-field approximation of the spatially-explicit model described later on and represents dynamics at the landscape scale, i.e. the variation in the amount of stands in each of the three states: forest F, infected I and recovering R. The total proportions of stands in each state sums to 1, such that $R = 1 - F - I$ and thereby allows to represent the dynamics with only two coupled differential equations (Fig. 1):

$$\frac{dF}{dt} = \gamma_1(1-F-I) - \beta F - \alpha f(I)[1-(1-I)^{24}]FI \tag{1a}$$

$$\frac{dI}{dt} = \beta F + \alpha f(I)[1-(1-I)^{24}]FI - \gamma_2 I \tag{1b}$$

As described above, infection of a forest stand F occurs in two ways, either by a spontaneous infection, whose probability is set by β, or by insects dispersing to a mature forest stand from an already infected stand I, set by α. Transmission of infectious agents in epidemiological models is usually approximated by mass action where the transmission probability is proportional to the prevalence of both susceptible and infected states (i.e. αFI). In our model host trees are stationary and the transmission probability corresponds to insect dispersal. Each stand is potentially surrounded by multiple infected stands, but a single successful dispersal event is sufficient to cause infection. The neighborhood of each stand is the closest 24 stands, and the probability at which a no-dispersal event occurs from all 24 of them is thus $(1-I)^{24}$. The probability of dispersal from *at least one* neighbor is $1-(1-I)^{24}$ (Fukś and Lawniczak, 2001; Guichard et al., 2003). This approximation allows us to implicitly include space, so a high proportion of infected forest stands means a high density of insects and indirectly a higher probability of infection.

The function $f(I)$ sets density-dependent dispersal as follows (Fig. S1, Hethcote and Levin, 1989):

$$f(I) = I^p \tag{2}$$

where p is a positive real number ≤ 1. Density-dependence increases as p gets closer to 1, indicating a lower infection probability when few stands are infected (Fig. S1). Note that the Allee effect and density-dependent emigration cannot be distinguished in the spatially-implicit model because the proportion of infected stands in the arrival stand is the same as in the neighborhood of source stand.

2.1.2. Spatially-explicit model formulation

We run a spatially-explicit model to investigate the effect of local dispersal on the infection dynamics. The *total* proportion of the lattice in each state is equivalent to the proportion modeled by the mean-field model. During one iteration of the model, each stand of the lattice may undergo a state transition according to the following rules:

$$F \rightarrow I \text{ if } \beta \geq h \tag{3a}$$

$$F \rightarrow I \text{ if } \alpha f(I) \geq h \tag{3b}$$

$$I \rightarrow R \text{ if } \gamma_2 \geq h \tag{3c}$$

$$R \rightarrow F \text{ if } \gamma_1 \geq h \tag{3d}$$

where h is a uniformly distributed random number between 0 and 1. Dispersal depends on the proportion of infected stands in the immediate neighborhood. We repeat infection trials for each of the infected neighboring stands (thereby explaining why I appears only once in the equation, while it appears twice in the spatially-implicit dispersal function – (2)), but only one successful dispersal event is enough to cause an infection. The spatially-explicit version allows to differentiate the two types of density-dependence described above.

Immigration Density-dependent immigration occurs when the infection probability is affected by the proportion of infected stands surrounding the arrival stand (Fig. S2). $\bar{I}_F$ represents the proportion of infected stands in the neighborhood centered on arrival stand. The infection probability is consequently:

$$f(I)_{Imm} = \bar{I}_F{}^p \tag{4}$$

Emigration Density-dependent emigration occurs when the infection probability is affected by the proportion of infected stands surrounding the stands of origin (Fig. S2). $\bar{I}_I$ represents the proportion of infected stands in the neighborhood centered around an origin stand. The infection probability is consequently:

$$f(I)_{Emi} = \bar{I}_I{}^p \tag{5}$$

2.2. Model implementation and analysis

We compare the spatially-implicit and -explicit versions of the FIRF model with numerical simulations and specifically study the impact of dispersal α and density-dependence p parameters on occurrence, frequency and amplitude of outbreaks. We are interested by the massive eruptions of insect damages at the regional scale, not the local scale. We consequently define outbreaks as sudden peaks in the proportion of infected stands at the regional scale. These could be cyclic, or not. Based on preliminary simulations, we identify outbreaks as events when more than 10% of the landscape is in the infected state. We record the minimum and maximum proportion of infected stands I during each simulation. Furthermore, if outbreaks occur, we identify whether they are cyclic with regular return intervals, or episodic with irregular intervals. We calculate the spectral frequency with a Fast Fourier Transform and smooth the data with a window of 10 periodicities to determine the outbreak interval. The dominant period (the reciprocal of the frequency) that has the highest spectral power contributes most to the oscillations observed in the time series. We compute the average dominant period of all repetitions above the threshold under the same parameters. All analyses were performed in the R environment (R Core Team, 2012).

We present the results from simulations without ($\beta = 0$) and with spontaneous infections ($0.00025 < \beta < 0.005$). Parameters α and p are varied $0 - 1$ in increments of 0.05 (Table S1), while β is varied $0 - 0.005$ by increments of 0.00025. The minimum time to reach mature forest in North American boreal forests range is 40 years (Burns and Honkala, 1990), and therefore we set γ_1 to 1/40. The infection duration at the stand scale varies regionally from 1 to 25 years (Gray, 2013). Severe defoliation usually occurs after a few years of light defoliation, tree mortality usually begins in the third to fifth year of severe defoliation, and full mortality occurs after around 10 years, when the tree is completely defoliated and unable to photosynthesize (MacLean, 1980). Based on this information we set γ_2 to 1/3, based on the minimum observed number of years for an infection to kill a forest stand. Note that outbreaks can also be found with longer time before mortality, although they are found in a more restricted parameter space. Both spatially-implicit and -explicit simulations were run for 20,000 time steps and we discarded the first transient 1000 steps. Each time step represents one year. The initial proportions are $F = 0.4$, $I = 0.1$ and $R = 0.5$.

2.2.1. Spatially-implicit model

Local equilibrium analysis is performed to identify the critical conditions required for the occurrence of damped or sustained oscillations at different parameter values (Fig. 2, Soetaert, 2009). Local equilibrium analysis consists of evaluating the Jacobian matrix at the positive equilibrium points. Oscillations occur if the eigenvalues of the Jacobian are complex. Because the equations with density-dependent dispersal function $f(I)$ (Eq. (2)) cannot be solved analytically, we use numerical local stability analysis instead of analytical. When $p = 0$ and $I^0 = 1$, the model with density-dependent dispersal reduces to the density-independent

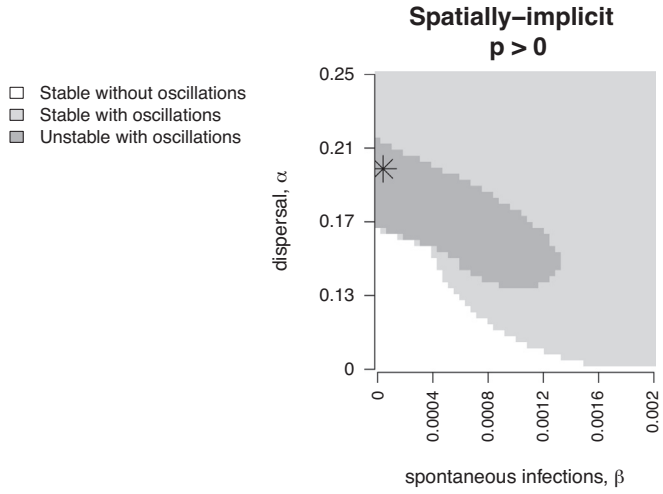

Fig. 2. The presence of cyclic outbreaks of the density-dependent spatially-implicit model under different strengths of β and α probabilities. At low parameter values the dynamics are stable (negative eigenvalues, white). At higher dispersal α the dynamics become unstable with oscillations (complex eigenvalues with positive real parts, dark grey). At higher dispersal β and α the dynamics are stable with damped oscillations (complex eigenvalues with negative real parts, light grey). The parameters of Fig. 3 are indicated by the black star. These density-dependent results can be compared to the local equilibrium results from the density-independent model with global mixing, supplementary materials Section S1.

model with global mixing in dispersal (αFI). The local equilibrium analysis with global mixing and density-independent dispersal are presented in Supplementary materials Section S1. We numerically simulate the spatially-implicit model with a Runge–Kutta fourth-order integration with a time step of 0.1.

2.2.2. Spatially-explicit model

We use a square lattice of 100^2 cells with periodic boundary conditions (torus). We initiate the lattice with the same proportions of states as the spatially-implicit model, distributed randomly in space. In each time step (year) we randomly select 100^2 stands and update their states. A stand may therefore have no or multiple state changes per stand in a single time step. This asynchronous updating method approximates continuous mean-field dynamics (Durrett and Levin, 1994). We run 20 stochastic simulations for each set of parameters.

We characterize the spatial structure of clustered infected stands, and measure if these infection patches display a range of different sizes. The log–log slope of the size-frequency distributions can be fitted with a power-law relationship, and its exponent reflects how the size of infection patches is related to their frequency. The frequency distribution of many ecological phenomena display such scale-free behaviour (Pascual and Guichard, 2005). Human epidemics have been reported to exhibit power-law scaling (Rezende and Anderson, 1997). We define an infection patch as the spatially contiguous collection of infected stands that are connected by any of their 8 closest neighbors (Moore neighborhood). The size of an infection patch is therefore the number of contiguous infected stands that constitutes it. We select the 100 years with the highest proportion of infected stands I and calculate patch size for all outbreaks in each of these years. Subsequently, we average the patch size data for the 100 years to compute the frequency distribution of infected stands per year. We then calculate the exponent of the relationship using a maximum likelihood estimator (Clauset et al., 2009).

3. Results

The FIRF models produce outbreaks in certain regions of parameter space and both with and without spontaneous infection ($\beta > 0$ or $\beta = 0$). In general, the conditions required to observe outbreaks differ between the spatially-implicit and -explicit models (Table 1, Fig. 3). The spatially-implicit model is deterministic while the spatially-explicit one is stochastic, which might explain the difference between them. We thus investigate if the stochastic dynamics itself causes outbreaks and examine the spatially-explicit model under global dispersal by selecting random stands to which dispersal occurred. No outbreaks were observed under global dispersal (results not shown), indicating that local dispersal between neighboring stands causes outbreaks, not stochastic dynamics.

Density-dependent dispersal promotes the occurrence of outbreaks in both local stability analysis (Supplementary materials Section S1) and simulations in the spatially-implicit model (Eqs. (1a) and (1b)). With density-independent dispersal ($p = 0$, Eq. (2)), there are damped oscillations (complex eigenvalues with negative real parts, results not shown). With density-dependent dispersal ($p > 0$) there are both unstable and stable dynamics in different regions in parameter space (Fig. 2). On the bifurcation boundary between the positive and negative eigenvalues there should be eigenvalues with zero real parts which indicate cyclic outbreaks. In spatially-implicit numerical simulations up to half of the landscape can become infected simultaneously during outbreaks (Fig. 3A, B for example simulations). With density-independent dispersal there are damped oscillations ($p = 0$, Fig. 3A) and with density-dependent dispersal there are sustained cyclic outbreaks ($p > 0$, Fig. 3B). Outbreaks are observed under certain conditions of dispersal, namely when $0.4 < p < 0.5$ (Fig. 5A) and $0.1 < \alpha < 0.3$ (Fig. 5D). Without spontaneous stand infection $\beta = 0$, there are no outbreaks in the spatially-implicit model (dotted lines in Fig. 5A, D).

Outbreaks in the spatially-explicit model occur at the same parameters as in the spatially-implicit model, but also in larger regions of parameter space (Eqs. (3a)–(3d), Fig. 3C, D for example simulations). With emigration-driven dispersal up to 30% of the area is infected at the same time (Fig. 5C) and with immigration-driven dispersal outbreaks are smaller. Spatially-explicit simulations are less sensitive to the strength of density-dependent dispersal p (Fig. 5B, C) and outbreaks occur when strength of dispersal $\alpha > 0.1$ (Fig. 5E, F). In the absence of spontaneous infection sustained outbreaks occur in smaller regions of parameter space (Figs. S3 and S5B, C, E, F). Note also that outbreaks can also be found with longer time before mortality (i.e. $\gamma_2 < 1/3$, although they are found in a more restricted parameter space.

Dispersal affects if outbreaks are cyclic (periodic) or irregular and the number of years between outbreaks (return interval). In both spatially-implicit and explicit models, outbreaks occur every 30–40 years at low values of density-dependence p (Fig. 6A–C) and moderate dispersal α (Fig. 6D–F). Spatially-explicit models produce longer cycles with stronger density-dependence p and stronger dispersal $\alpha < 0.6$–0.8 removes all cyclic outbreaks.

The spatially-explicit models generate clusters of infected stands (Fig. 4A, B). The size of these infection patches is larger when there are few spontaneous infections and moderate dispersal; when rare infections disperse through large areas of undisturbed susceptible forest (in terms of number of infection patches, Fig. 7A, B). The size-frequency distributions of infection patches indicate that the FIRF model has few large and many small infection patches, and the slope of the relationship is dependent on the parameters and model type. With low dispersal ($0.1 < \alpha < 0.2$), the slope is shallower, producing a higher proportion of large and fewer smaller infection patches (Fig. 7C, D). Emigration-driven dispersal produces larger infection patches for most parameter sets.

4. Discussion

We developed a process-based landscape model that simulates spatiotemporally synchronized insect outbreaks. Our model is

Table 1
Conclusions from comparing the results from both spatially-implicit and -explicit FIRF models under different types of density-dependence. 'Yes' indicates that outbreaks occur under at least some parameter values. For the local stability analysis of the spatially-implicit model, outbreaks (damped or sustained oscillations) are indicated by the presence of complex eigenvalues. Outbreak cyclicity is assessed by numerical simulations.

Model	Density-dependence	One outbreak	Cyclic outbreaks	Patchy landscapes
Spatially-implicit	$p = 0$	Yes	No	–
	$p > 0$	Yes	Yes	–
Spatially-explicit	$p = 0$	–	Yes	Yes
Immigration	$p > 0$	–	Yes	Yes
Emigration	$p > 0$	–	Yes	Yes

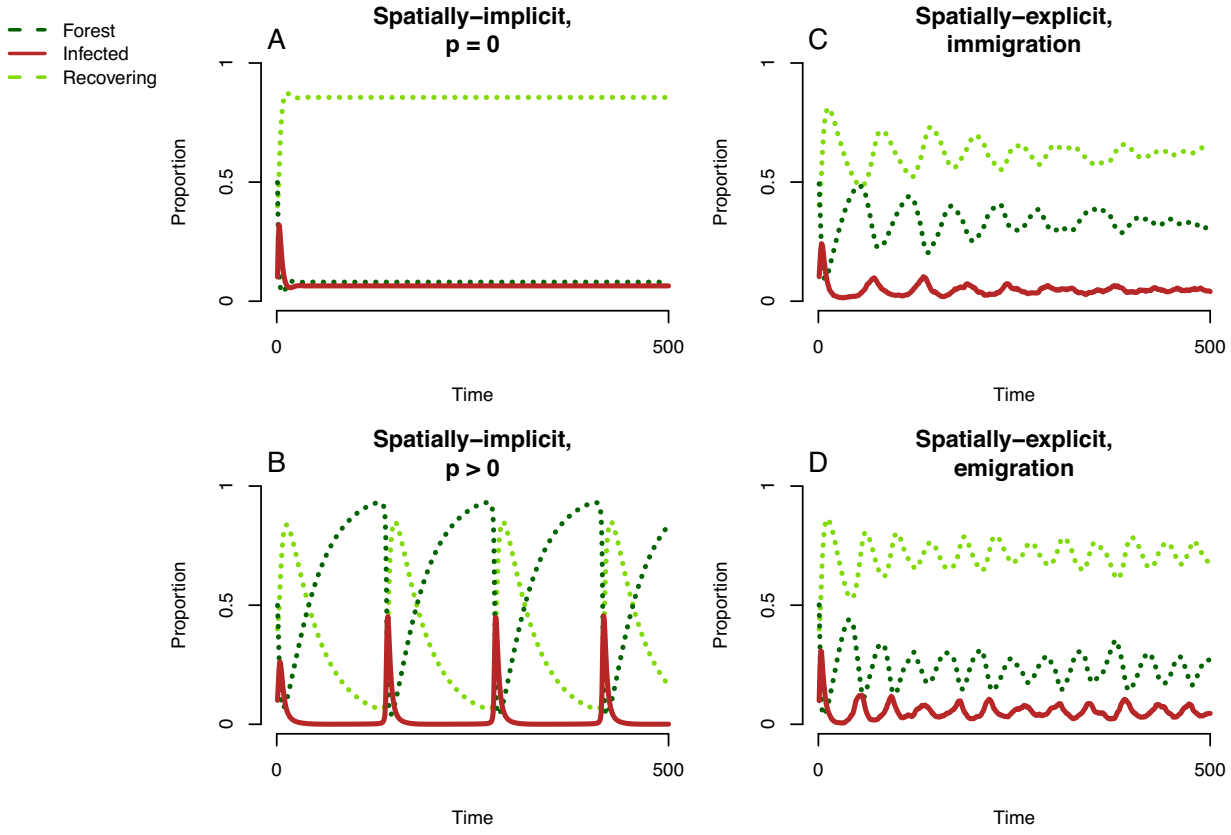

Fig. 3. Examples of FIRF model simulations with the proportion of each forest state over time. (A) Spatially-implicit model with density-independent dispersal ($p = 0$) and (B) density-dependent dispersal ($p > 0$). (C) Spatially-explicit immigration-driven density-dependent dispersal ($p > 0$). (D) spatially-explicit emigration-driven dispersal model ($p > 0$). The parameters used are $\alpha = 0.2$, $\beta = 0.001$, $\gamma_1 = 1/40$, $\gamma_2 = 1/3$ and $p = 0.4$. We show the dynamics with $\beta = 0$ in Fig. S3.

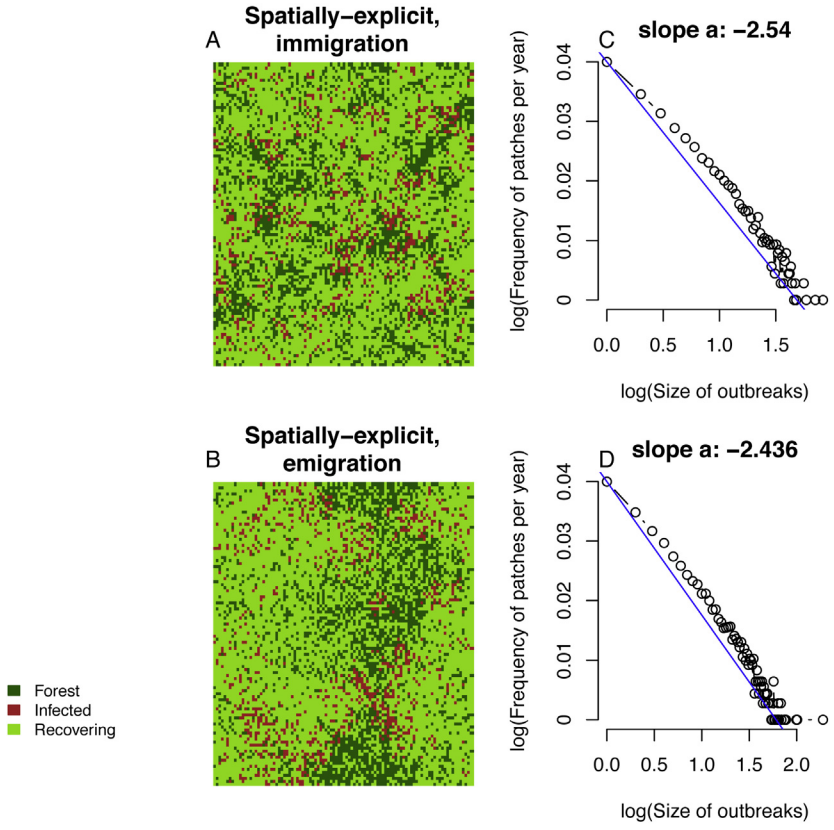

Fig. 4. The spatial distribution of stands in one year during the simulation runs in Fig. 3 (A, immigration-driven dispersal, B, emigration-driven dispersal) and the corresponding power-law slope (C, immigration-driven dispersal, D, emigration-driven dispersal). The number and sizes of infection patches that were used to calculate the power law was averaged from the 100 years with highest infection prevalence in each simulation. The map has the same legend as in 3 and the landscape scale is 100^2 stands.

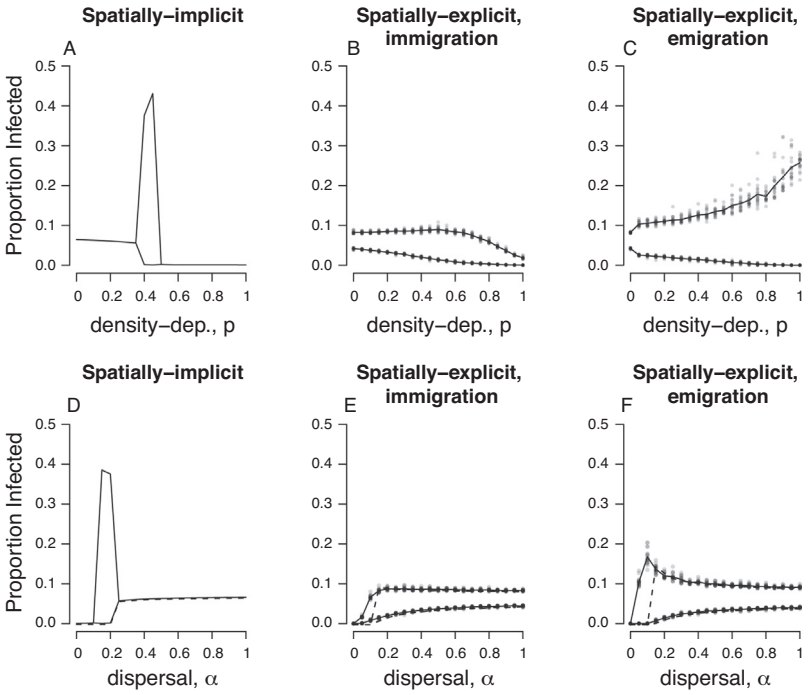

Fig. 5. The minimum and maximum proportion of infected area per simulation as a function of density-dependence p (A–C) and dispersal α (D–F). Solid lines indicate averages from simulations with $\beta = 0.0001$ and points indicate values from each simulation. Dotted lines indicate $\beta = 0$. For clarity we do not show the values of each simulation when $\beta = 0$. (A, D) Spatially-implicit model. (B, E) Spatially-explicit immigration-driven dispersal. (C, F) Spatially-explicit emigration-driven dispersal. Other parameters are the same as in Fig. 3. The proportion infected is calculated after the transient period of 1000 years.

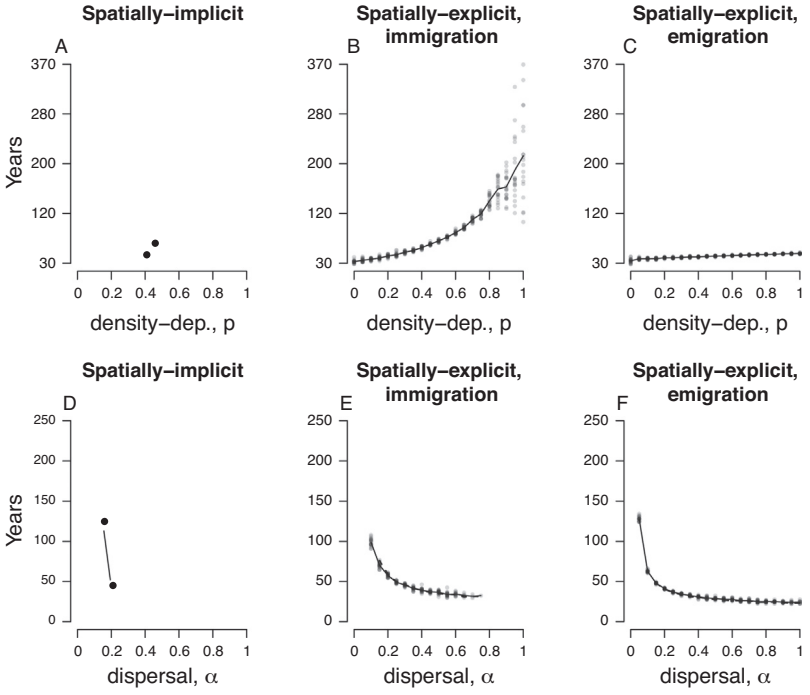

Fig. 6. The length of outbreak return intervals as a function of density-dependence p (A–C) and dispersal α (D–F). Solid lines indicate averages from simulations with $\beta = 0.0001$ and points indicate values from each simulation. Dotted lines indicate $\beta = 0$. For clarity we do not show the values of each simulation when $\beta = 0$. Missing lines indicate that there is no periodicity. (A, D) Spatially-implicit model. (B, E) Spatially-explicit immigration-driven dispersal. (C, F) Spatially-explicit emigration-driven dispersal. Other parameters are the same as in Fig. 3.

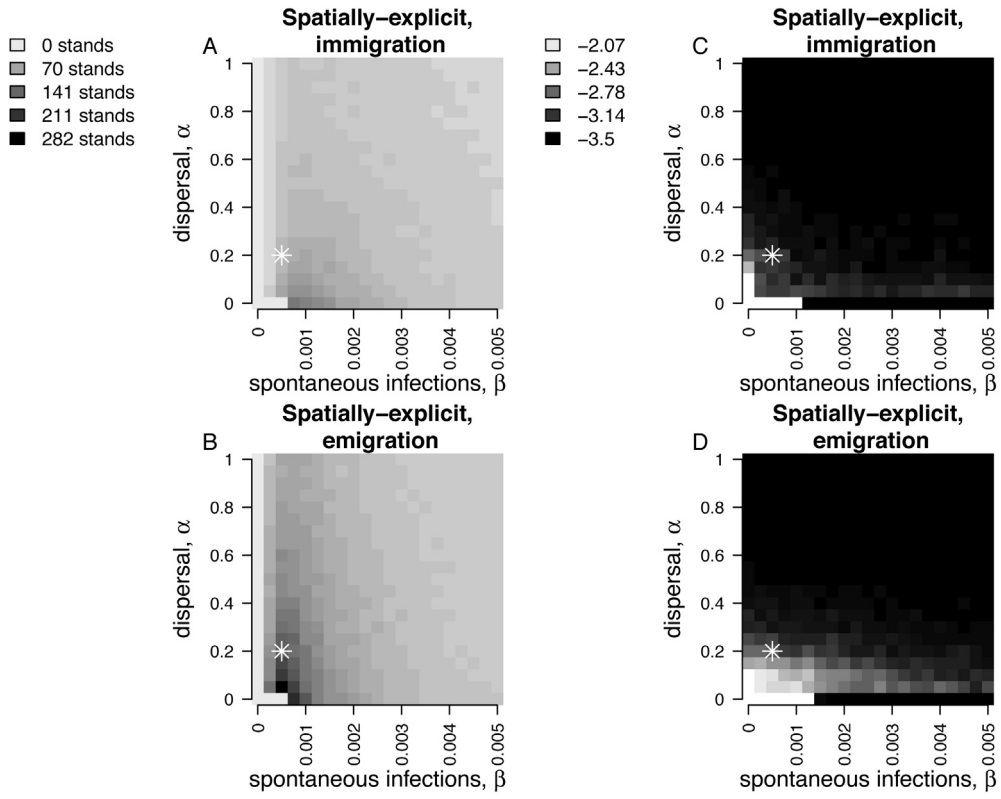

Fig. 7. The average size of the largest infection patch (A, C, maximum number of stands per infection patch, average for 20 repetitions) and the average exponent of the power-law slope (C, D, average for 20 repetitions). A shallower slope indicates a higher proportion of larger infection patches, which would be expected when there are large outbreaks. The parameters used in Fig. 3 are indicated by the star.

inspired by Levins (1969) metapopulation model, but instead of presence and absence of species in habitat patches we simulate presence or absence of pest infections in forest stands, drawing inspiration from epidemiological models. Our framework, therefore, reflects observed endemic and epidemic periods as well as outbreak epicenters (Cooke et al., 2007). The process-based landscape FIRF model proposed here generates outbreak intervals comparable to real outbreaks, around 30 years (Boulanger et al., 2012). We find that dispersal alone in some regions of parameter space produces outbreaks, even without spontaneous infection. This implies that dispersal is sufficient to cause synchronous outbreaks, and that other processes may not be instrumental in explaining cyclic outbreaks. While damped oscillations are not sustained oscillations *per se*, they can result in quasi-periodic fluctuations when further amplified by environmental stochasticity (Peltonen et al., 2002; Ripa and Ranta, 2007). Our results highlight the necessity of explicitly modeling the spatial dimension when studying landscape-scale insect outbreaks, demonstrating the importance of dispersal in the emergence of insect outbreaks.

The model generates outbreaks with both spatially-implicit and -explicit dispersal, but through different processes. Density-dependent dispersal is necessary for the onset of outbreaks in the spatially-implicit model, but not in the spatially-explicit one, meaning that outbreaks arise from the spatial implementation itself. Even though dispersal is stochastic in each stand in the spatially-explicit model, on a landscape-scale outbreaks recur with regular intervals. The spatially-explicit model formulation is more robust because the same results are obtained over a wider range of parameter values. Emigration-driven density-dependent dispersal produced larger outbreaks, suggesting that stand-specific resource-limitations can cause landscape outbreaks and should be further studied.

Our metapopulation-epidemiological FIRF model presents certain advantages over population-based models. The biggest advantage is that it does not require estimates of insect densities, which are difficult to obtain for entire landscapes, in particular for endemic densities. While it is beyond the scope of this study to validate the model with observed outbreak data, this model could eventually be parameterized using aerial observation data (as in Bouchard and Auger, 2014) to validate dispersal assumptions, and to explore landscape-scale outbreak causes further. Another advantage is that local population dynamics are represented only by their stand impact, so the FIRF model requires fewer adjustable parameters than a population model. Future studies could expand on the proposed theoretical framework to advance the understanding of forest insect landscape dynamics. For example, one could easily investigate the effect of landscape heterogeneity and connectivity on the dynamics of outbreaks. The effect of future environmental conditions on insect outbreak dynamics could also be evaluated by exploring different parameter values for forest mortality, γ_2, and recovery, γ_1. Although our model formulation was inspired by the spruce budworm, the parameter exploration suggests that our model is quite flexible and can be used to study various forest insect defoliators with different life histories and population characteristics. Not all insect defoliators display outbreaks (Liebhold and Kamata, 2000), just like some sets of parameters do not produce outbreaks.

We show that spatial models are preferable to study outbreaks, which has practical implications for epidemiology because a correct model formulation is essential to implement effective vaccination programs. For example, an individual-based model fit observed rabies occurrence data better than a classical mean-field formulation, and could offer more effective spatial vaccination strategies (Eisinger and Thulke, 2008). There are spatial epidemiological models with a variable transmission probability as

implemented here, but they ignore recurrent infections and only follow the dynamics of one outbreak (but see Silva and Monteiro, 2014). Our model improves understanding of dispersal on recurrent landscape outbreaks, which is important for many epidemics, including forest insects.

5. Conclusion

Current forest management practices to control insect outbreaks are spatially-implicit, so the proposed spatially-explicit landscape model could improve management interventions. The model could be useful to elaborate outbreak management strategies for three reasons. First, it is a process-based model which is advantageous because it is driven by documented ecological processes and can be used under changing conditions (Cuddington et al., 2013). Second, the model is formulated at the scale at which landscape management occurs, i.e., forest stands, which is advantageous both theoretically and practically (Meentemeyer et al., 2012; Stevens et al., 2007). Third, due to its similarity to the highly applied discipline of epidemiology, our ecological metapopulation model opens new perspectives towards managing insect outbreaks. Here we show that lower dispersal probabilities produce smaller outbreaks, both in individual outbreak size and in total infected area. Management strategies could weaken outbreaks by minimizing insect dispersal through modifying the connectivity of susceptible mature forest stands, logging and/or establishment of non-host forest stands. Future versions of the model could be coupled with epidemiology-inspired management practices and explore their effects on outbreaks. Our process-based landscape FIRF framework suggests that interventions beyond the stand scale could lead to effective forest management by interfering with the spatial processes inherent in insect outbreaks.

Acknowledgements

Funding was provided by the Forest Complexity modeling program, Natural Sciences and Engineering Research Council of Canada – Collaborative Research and Training Experience and Discovery programmes, Canada Research Chairs, Université du Québec à Montréal and a Doctoral Research Fellowship from the Fonds de recherche du Québec – Nature et technologies. Thanks to Yan Boulanger, Lukas Seehausen and Veronique Martel for spruce budworm discussions, and to Christian Messier and Frédéric Guichard. Thanks to Amael Le Squin, Renato Silva, Alyssa Butler and numerous reviewers for comments on the manuscript.

Appendix A. Supplementary data

Supplementary data associated with this article can be found, in the online version, at http://dx.doi.org/10.1016/j.ecocom.2017.04.004.

References

Anderson, R.M., May, R.M., 1979. Population biology of infectious disease: Part I. Nature 280, 361–367.
Bergeron, Y., Leduc, A., Morin, H., Joyal, C., 1995. Balsam fir mortality following the last spruce budworm outbreak in northwestern Quebec. Can. J. For. Res. 25, 1375–1384.
Bjørnstad, O.N., Grenfell, B.T., 2001. Noisy clockwork: time series analysis of population fluctuations in animals. Science 293, 638–643.
Bjørnstad, O.N., Peltonen, M., Liebhold, A.M., Baltensweiler, W., 2002. Waves of larch budmoth outbreaks in the European Alps. Science 298, 1020–1023.
Blais, J.R., 1958. The vulnerability of balsam fir to spruce budworm attack in northwestern Ontario, with special reference to the physiological age of the tree. For. Chron. 34, 405–422.
Bouchard, M., Auger, I., 2014. Influence of environmental factors and spatio-temporal covariates during the initial development of a spruce budworm outbreak. Landsc. Ecol. 29, 111–126.
Boulanger, Y., Arseneault, D., Morin, H., Jardon, Y., Bertrand, P., Dagneau, C., 2012. Dendrochronological reconstruction of spruce budworm (*Choristoneura fumiferana*) outbreaks in southern Quebec for the last 400 years. Can. J. For. Res. 42, 1264–1276.
Bowler, D.E., Benton, T.G., 2005. Causes and consequences of animal dispersal strategies: relating individual behaviour to spatial dynamics. Biol. Rev. 80, 205–225.
Boyd, I.L., Freer-Smith, P.H., Gilligan, C.A., Godfray, H.C.J., 2013. The consequence of tree pests and diseases for ecosystem services. Science 342, 1235773.
Burns, R.M., Honkala, B.H., 1990. Silvics of North America: 1. Conifers; 2. Hardwoods. Agriculture Handbook 654, vol. 2. U.S. Department of Agriculture, Forest Service, Washington, DC.
Clauset, A., Shalizi, C., Newman, M.E.J., 2009. Power-law distributions in empirical data. SIAM Rev. 51, 661–703.
Cooke, B.J., Nealis, V.G., Régnière, J., 2007. Insect defoliators as periodic disturbances in northern forest ecosystems. In: Johnson, E., Miyanishi, K. (Eds.), Plant Disturb. Ecol. Process Response. Elsevier, Burlington, MA, USA, pp. 487–525.
Cuddington, K.M., Fortin, M.J., Gerber, L.R., Hastings, A., Liebhold, A.M., O'Connor, M., Ray, C., 2013. Process-based models are required to manage ecological systems in a changing world. Ecosphere 4, 1–12.
Durrett, R., Levin, S.A., 1994. The importance of being discrete (and spatial). Theor. Popul. Biol. 46, 363–394.
Earn, D.J.D., Rohani, P., Grenfell, B.T., 1998. Persistence, chaos and synchrony in ecology and epidemiology. Proc. R. Soc. B: Biol. Sci. 265, 7–10.
Eisinger, D., Thulke, H., 2008. Spatial pattern formation facilitates eradication of infectious diseases. J. Appl. Ecol. 45, 415–423.
Elton, C.S., 1924. Periodic fluctuations in the number of animals: their causes and effects. J. Exp. Biol. 2, 119–163.
Erdle, T.A., Maclean, J.E., 1999. Stand growth model calibration for use in forest pest impact assessment. For. Chron. 75, 141–152.
Evans, M.R., Norris, K.J., Benton, T.G., 2012. Predictive ecology: systems approaches. Philos. Trans. R. Soc. B: Biol. Sci. 367, 163–169.
Filipe, J.A.N., Cobb, R.C., Meentemeyer, R.K., Lee, C.A., Valachovic, Y.S., Cook, A.R., Rizzo, D.M., Gilligan, C.A., 2012. Landscape epidemiology and control of pathogens with cryptic and long-distance dispersal: sudden oak death in northern Californian forests. PLoS Comput. Biol. 8, e1002328.
Filipe, J.A.N., Maule, M., 2004. Effects of dispersal mechanisms on spatio-temporal development of epidemics. J. Theor. Biol. 226, 125–141.
Fleming, R.A., 2000. Climate change and insect disturbance regimes in Canada's boreal forests. World Resour. Rev. 12, 521–555.
Fuentes, M., Kuperman, M.N., Fuentes, M.A., 1999. Cellular automata and epidemiological models with spatial dependence. Physica A 267, 471–486.
Fukś, H., Lawniczak, A.T., 2001. Individual-based lattice model for spatial spread of epidemics. Discret. Dyn. Nat. Soc. 6, 191–200.
Gray, D.R., 2008. The relationship between climate and outbreak characteristics of the spruce budworm in eastern Canada. Clim. Change 87, 361–383.
Gray, D.R., 2013. The influence of forest composition and climate on outbreak characteristics of the spruce budworm in eastern Canada. Can. J. For. Res. 1195, 1181–1195.
Greenbank, D., 1980. Spruce budworm (Lepidoptera: Tortricidae) moth flight and dispersal: new understanding from canopy observations, radar, and aircraft. Mem. Entomol. Soc. Canada 112, 1–49.
Grenfell, B.T., Harwood, J., 1997. (Meta)population dynamics of infectious diseases. Trends Ecol. Evol. 12, 395–399.
Guichard, F., Halpin, P.M., Allison, G.W., Lubchenco, J., Menge, B.A., 2003. Mussel disturbance dynamics: signatures of oceanographic forcing from local interactions. Am. Nat. 161, 889–904.
Gustafson, E.J., 2013. When relationships estimated in the past cannot be used to predict the future: using mechanistic models to predict landscape ecological dynamics in a changing world. Landsc. Ecol. 28, 1429–1437.
Hanski, I., 1998. Metapopulation dynamics. Nature 396, 41–49.
Hardy, Y., Lafond, A., Hamel, L., 1983. The epidemiology of the current spruce budworm outbreak in Quebec. For. Sci. 29, 715–725.
Hethcote, H.W., 1976. Qualitative analyses of communicable disease models. Math. Biosci. 28, 335–356.
Hethcote, H.W., Levin, S.A., 1989. Periodicity in epidemiological models. In: Gross, L., Hallam, T.G., Levin, S.A. (Eds.), Appl. Math. Ecol. Springer, Berlin, pp. 193–211.
Ims, R.A., Yoccoz, N.G., Hagen, S.B., 2004. Do sub-Arctic winter moth populations in coastal birch forest exhibit spatially synchronous dynamics? J. Anim. Ecol. 73, 1129–1136.
James, P.M.A., Fortin, M.J., Sturtevant, B.R., Fall, A., Kneeshaw, D., 2010. Modelling spatial interactions among fire, spruce budworm, and logging in the boreal forest. Ecosystems 14, 60–75.
Johnson, D.M., Liebhold, A.M., Tobin, P.C., Bjørnstad, O.N., 2006. Allee effects and pulsed invasion by the gypsy moth. Nature 444, 361–363.
Keane, R.E., McKenzie, D., Falk, D., Smithwick, E., Miller, C., Kellogg, L.K., 2015. Representing climate, disturbance, and vegetation interactions in landscape models. Ecol. Model. 309–310, 33–47.
Keeling, M.J., Rohani, P., 2008. Modeling Infectious Diseases in Humans and Animals. Princeton University Press, Princeton, NJ.
Keeling, M.J., Woolhouse, M.E.J., May, R.M., Davies, G., Grenfell, B.T., 2003. Modelling vaccination strategies against foot-and-mouth disease. Nature 421, 136–142.

Kéfi, S., Rietkerk, M., Alados, C., Pueyo, Y., Papanastasis, V.P., ElAich, A., De Ruiter, P.C., 2007. Spatial vegetation patterns and imminent desertification in Mediterranean arid ecosystems. Nature 449, 213–217.
Kermack, W.O., McKendrick, A.G., 1927. A contribution to the mathematical theory of epidemics. Proc. R. Soc. A: Math. Phys. Eng. Sci. 115, 700–721.
Kleczkowski, A., Gilligan, C.A., Bailey, D.J., 1997. Scaling and spatial dynamics in plant-pathogen systems: from individuals to populations. Proc. R. Soc. B: Biol. Sci. 264, 979–984.
Levins, R., 1969. Some demographic and genetic consequences of environmental heterogeneity for biological control. Bull. Ecol. Soc. Am. 15, 237–240.
Liebhold, A.M., Kamata, N., 2000. Introduction – are population cycles and spatial synchrony a universal characteristic of forest insect populations? Popul. Ecol. 42, 205–209.
Liebhold, A.M., Koenig, W.D., Bjørnstad, O.N., 2004. Spatial synchrony in population dynamics. Annu. Rev. Ecol. Evol. Syst. 35, 467–490.
MacLean, D.A., 1980. Vulnerability of fir-spruce stands during uncontrolled spruce budworm outbreaks: a review and discussion. For. Chron. 56, 213–221.
Maclean, J.E., Olstaff, D.P., 1989. Pattern of balsam fir mortality caused by an uncontrolled budworm outbreak. Can. J. For. Res. 19, 1087–1095.
Malamud, B.D., Morein, G., Turcotte, D.L., 1998. Forest fires: an example of self-organized critical behavior. Science 281, 1840–1842.
McCullough, D.G., Werner, R.A., Neumann, D., 1998. Fire and insects in northern and boreal forest ecosystems of North America. Annu. Rev. Entomol. 43, 107–127.
Meentemeyer, R.K., Haas, S.E., Václavík, T., 2012. Landscape epidemiology of emerging infectious diseases in natural and human-altered ecosystems. Annu. Rev. Phytopathol. 50, 379–402.
Morin, H., Jardon, Y., Gagnon, R., 2007. Relationship between spruce budworm outbreaks and forest dynamics in eastern North America. In: Johnson, E., Miyanishi, K. (Eds.), Plant Disturb. Ecol. Process Response. Elsevier, New York, pp. 555–577.
Nealis, V.G., Régnière, J., 2004. Fecundity and recruitment of eggs during outbreaks of the spruce budworm. Can. Entomol. 136, 591–604.
Neri, F.M., Bates, A., Füchtbauer, W.S., Pérez-Reche, F.J., Taraskin, S.N., Otten, W., Bailey, D.J., Gilligan, C.A., 2011. The effect of heterogeneity on invasion in spatial epidemics: from theory to experimental evidence in a model system. PLoS Comput. Biol. 7, 1–7.
Neri, F.M., Pérez-Reche, F.J., Taraskin, S.N., Gilligan, C.A., 2011. Heterogeneity in susceptible-infected-removed (SIR) epidemics on lattices. J. R. Soc. Interface 8, 201–209.
NFS, 2013. Silviculture – Quick Facts. In: National Forestry Database (NFD)National Forest Service, Canada.
Pascual, M., Guichard, F., 2005. Criticality and disturbance in spatial ecological systems. Trends Ecol. Evol. 20, 88–95.
Peltonen, M., Liebhold, A.M., Bjørnstad, O.N., Williams, D.W., 2002. Spatial synchrony in forest insect outbreaks: roles of regional stochasticity and dispersal. Ecology 83, 3120–3129.
Peters, D.P.C., Pielke, R.A., Bestelmeyer, B.T., Allen, C.D., Munson-mcgee, S., Havstad, K.M., 2004. Cross-scale interactions, nonlinearities, and forecasting catastrophic events. Proc. Natl. Acad. Sci. U. S. A. 101, 15130–15135.
R Core Team, 2012. R: A Language and Environment for Statistical Computing, http://www.r-project.org/.
Régnière, J., Delisle, J., Pureswaran, D.S., Trudel, R., 2013. Mate-finding Allee effect in spruce budworm population dynamics. Entomol. Exp. Appl. 146, 112–122.
Rezende, E.L., Anderson, R.M., 1997. On the critical behaviour of simple epidemics. Proc. R. Soc. B: Biol. Sci. 264, 1639–1646.
Rhodes, C.J., Anderson, R.M., Rezende, E.L., 1998. Forest-fire as a model for the dynamics of disease epidemics. J. Franklin Inst. 335, 199–211.
Riley, S., 2007. Large-scale spatial-transmission models of infectious disease. Science 316, 1298–1301.
Ripa, J., Ranta, E., 2007. Biological filtering of correlated environments: towards a generalised Moran theorem. Oikos 116, 783–792.
Royama, T., 1984. Population dynamics of the spruce budworm *Choristoneura fumiferana*. Ecol. Monogr. 54, 429–462.
Royama, T., MacKinnon, W., Kettela, E., Carter, N., Hartling, L., 2005. Analysis of spruce budworm outbreak cycles in New Brunswick, Canada, since 1952. Ecology 86, 1212–1224.
Silva, H.A.L.R., Monteiro, L.H.A., 2014. Self-sustained oscillations in epidemic models with infective immigrants. Ecol. Complex. 17, 40–45.
Soetaert, K., 2009. rootSolve: Nonlinear Root Finding, Equilibrium and Steady-State Analysis of Ordinary Differential Equations. R-Package Version 1.6.
Staver, A.C., Levin, S.A., 2012. Integrating theoretical climate and fire effects on savanna and forest systems. Am. Nat. 180, 211–224.
Stevens, C.J., Fraser, I., Mitchley, J., Thomas, M.B., 2007. Making ecological science policy-relevant: issues of scale and disciplinary integration. Landsc. Ecol. 22, 799–809.
Tenow, O., Nilssen, A.C., Bylund, H., 2012. Geometrid outbreak waves travel across Europe. J. Anim. Ecol. 82, 84–95.
Williams, D.W., Liebhold, A.M., 2000. Spatial synchrony of spruce budworm outbreaks in eastern North America. Ecology 81, 2753–2766.